

Optimal estimator for the amplitude of the bispectrum from IR sources

F. Lacasa¹★ and N. Aghanim¹★★

Institut d’Astrophysique Spatiale (IAS), Bâtiment 121, F-91405 Orsay (France); Université Paris-Sud 11 and CNRS (UMR 8617)

Abstract

We devise a fast and optimal estimator for the amplitude of the bispectrum of clustered Infrared (IR) point-sources. We show how this estimator can account for the cases of partial sky coverage and inhomogeneous noise. Expected detection significance are presented in terms of signal-to-noise, finding that the IR bispectrum will realistically be undetectable below 220 GHz with a Planck-like experiment; on the contrary detection may be achieved at, or above, 220 GHz especially if the CMB is removed. We also show how this estimator can be combined with estimators of radio and CMB non-Gaussianity to build up joint robust constraints. On the one hand, we find that, for a Planck-like experiment, CMB non-Gaussianity estimation can be decoupled from point-source contributions, unless few sources are masked. On the other hand, we find that the estimation of radio and IR non-Gaussianity are strongly coupled, which diminishes their separate detection significance.

Key words. Cosmology – CIB

1. Introduction

The measurement and study of high order moments has emerged as an important field in observational cosmology as it probes deviations from Gaussianity. For example, observing non-Gaussianity (NG) from the Cosmic Microwave Background (CMB) or the large scale structure would probe primordial NG dating back to the generation of cosmological perturbations ; this in turn would constrain severely primordial models generating these fluctuations (e.g. inflation). For example, a NG detection with the sensitivities of today’s experiments would rule out a whole class of inflation models, among which the standard single-field slow roll inflation (Acquaviva et al. 2003; Maldacena 2003; Creminelli & Zaldarriaga 2004).

The most popular form of primordial non-Gaussianity is the so-called ‘local’ type, parametrised by a factor f_{NL} , for which the Bardeen potential takes the form :

$$\Phi(\mathbf{x}) = \Phi_G(\mathbf{x}) + f_{NL} (\Phi_G(\mathbf{x})^2 - \langle \Phi_G(\mathbf{x})^2 \rangle) \quad (1)$$

where Φ_G is the Gaussian part of the potential. It is on this form of NG that most efforts have focused and that the tightest constraints were obtained. Indeed a fast estimators for f_{NL} was developed and applied to the CMB data (Komatsu et al. 2005, 2009, 2011). However at CMB frequencies, many contaminating signals are present, which typically have a non-Gaussian distribution. While the galactic emission is mainly confined to a defined area : the galactic plane, and may thus be masked, extra-galactic point-sources are present all over the sky and the faintest (below detection limits and confusion levels) are neither detected nor masked. These unresolved sources are therefore one potentially important source of secondary non-Gaussianity that needs to be estimated.

There are principally two populations of point-sources of interest for the CMB : radio-loud sources with strong magnetic

fields yielding synchrotron or free-free emission in the radio domain, and Dusty Star-Forming Galaxies (DSFGs) with thermal emission from dust heated by young star in the infrared (IR) domain. Radio galaxies can be considered randomly distributed on the sky (Toffolatti et al. 1998; González-Nuevo et al. 2005) at the CMB frequencies and thus have flat moments. Their skewness is related to their number counts as :

$$b_{PS} = \int S^3 \frac{dn}{dS} dS \quad (2)$$

where S is the source flux in Jy (b_{PS} may then be converted to CMB temperature elevation through Planck’s law, but is usually quoted in dimensionless units $\Delta T/T$ in the literature).

On the contrary, infrared galaxies are strongly clustered in dark matter halos, which typically enhances their correlation functions on large scales. Most recent CMB experiments, e.g. Planck (Planck Collaboration 2006), ACT (Das et al. 2011) and SPT (Keisler et al. 2011), are probing higher frequencies compared to previous missions so that the modeling and measurement of the infrared background becomes important. The Cosmic Infrared Background (CIB) and its anisotropies have indeed been detected and characterised at the power spectrum level at these frequencies (e.g. Hall et al. 2010; Planck Collaboration et al. 2011b; Viero et al. 2012).

Non-Gaussianity arising from point sources (radio or IR) is of particular importance for CMB studies, where maps are contaminated by foregrounds which are imperfectly subtracted by component separation methods. Therefore estimation of the primordial NG parameter f_{NL} may be contaminated by the point-source NG (Babich & Pierpaoli 2008; Lacasa et al. 2012). Measurement of the non-Gaussianity of point-sources could also be a new way to further constrain the respective models for their emission and/or spatial distribution.

A fast estimators for b_{PS} has been developed and applied to CMB data (Komatsu et al. 2005, 2009, 2011). Taking advantage of a prescription for the non-Gaussianity of IR source developed by (Lacasa et al. 2012), the goal of this article is to propose a

★ E-mail: Fabien.Lacasa@ias.u-psud.fr

★★ E-mail: Nabila.Aghanim@ias.u-psud.fr

fast estimator for the amplitude of the IR bispectrum. This can be used in non-Gaussianity studies to disentangle the primordial and foreground contributions so that measurements of both of them are unbiased.

The article is organised as follows : in section 2 we briefly recall the prescription for the bispectrum of IR sources and introduce the estimator for its amplitude, in section 3 we tackle the problems of partial sky coverage and anisotropic noise, in section 4 we present the expected signal-to-noise ratio (SNR) of detection at several frequencies, in section 5 we show how to combine this estimator with the ones used for the CMB and radio galaxies to produce a joint constraint of non-Gaussianity, and we conclude in section 6.

2. Bispectrum of IR sources

2.1. Bispectrum

Given a full-sky map of the temperature fluctuations $\Delta T(\mathbf{n})$ of some signal in direction \mathbf{n} , it can be decomposed in the spherical harmonic basis

$$a_{\ell m} = \int d^2\mathbf{n} Y_{\ell m}^*(\mathbf{n}) \Delta T(\mathbf{n}) \quad (3)$$

with the usual orthonormal spherical harmonics $Y_{\ell m}$

$$\int d^2\mathbf{n} Y_{\ell m}(\mathbf{n}) Y_{\ell' m'}^*(\mathbf{n}) = \delta_{\ell\ell'} \delta_{mm'} \quad (4)$$

The power spectrum C_ℓ of the signal is the 2-point correlation function in harmonic space given as :

$$\langle a_{\ell m} a_{\ell' m'}^* \rangle = C_\ell \delta_{\ell\ell'} \delta_{mm'} \quad (5)$$

The bispectrum $b_{\ell_1 \ell_2 \ell_3}$ is the 3-point correlation function in harmonic space:

$$\langle a_{\ell_1 m_1} a_{\ell_2 m_2} a_{\ell_3 m_3} \rangle = G_{\ell_1 \ell_2 \ell_3}^{m_1 m_2 m_3} \times b_{\ell_1 \ell_2 \ell_3} \quad (6)$$

with the Gaunt coefficient

$$G_{1,2,3} = \int d^2\mathbf{n} Y_{123}(\mathbf{n}) \quad (7)$$

$$= \sqrt{\frac{(2\ell+1)_{123}}{4\pi}} \begin{pmatrix} \ell_1 & \ell_2 & \ell_3 \\ 0 & 0 & 0 \end{pmatrix} \begin{pmatrix} \ell_1 & \ell_2 & \ell_3 \\ m_1 & m_2 & m_3 \end{pmatrix} \quad (8)$$

where $Y_i = Y_{\ell_i m_i}$. In the following the subscript 123 denotes the product of the corresponding variables e.g. $X_{123} \equiv X_1 X_2 X_3$. $G_{1,2,3}$ is zero unless the triplet (ℓ_1, ℓ_2, ℓ_3) follows the triangle inequalities and $m_1 + m_2 + m_3 = 0$.

The bispectrum estimator is :

$$\hat{b}_{123} = \frac{1}{N_{123}} \sum_{m_1, m_2, m_3} G_{1,2,3} a_1 a_2 a_3 \quad (9)$$

with

$$N_{\ell_1 \ell_2 \ell_3} = \frac{(2\ell+1)_{123}}{4\pi} \begin{pmatrix} \ell_1 & \ell_2 & \ell_3 \\ 0 & 0 & 0 \end{pmatrix}^2 \quad (10)$$

being the ‘number of modes’ for the (ℓ_1, ℓ_2, ℓ_3) triangle.

In the following, we note in bold the bispectrum which accounts for beam effect :

$$\mathbf{b}_{1,2,3} = b_{\ell_1 \ell_2 \ell_3} b_{\ell_1} b_{\ell_2} b_{\ell_3}$$

. We also note

$$C_\ell = C_\ell b_\ell^2 + C_\ell^{\text{noise}}$$

The power spectrum accounting for both the noise and the beam effects.

2.2. Optimal estimator of the amplitude of the bispectrum

The non-Gaussianity from radio sources at CMB frequencies is entirely characterised by a single parameter b_{PS} which can be estimated on a map (Komatsu et al. 2005). Hence the radio-source contamination to f_{NL} can be marginalised over. By contrast, the IR non-Gaussianity is more complicated and is characterised by the full bispectrum, whose estimation is computationally intensive (with $O(N_{\text{pix}}^{5/2})$ operations).

In this context, Lacasa et al. (2012) have proposed a full-sky analytical prescription to compute the bispectrum of extra-galactic sources from their number counts and power spectra. In this prescription, the bispectrum arising from a population of point sources writes :

$$b_{\ell_1 \ell_2 \ell_3}^{\text{PS}} = \alpha \sqrt{C_{\ell_1} C_{\ell_2} C_{\ell_3}} \quad (11)$$

with C_ℓ being the power spectrum of the considered point sources, and

$$\alpha = \frac{\int S^3 \frac{dN}{dS} dS}{\left(\int S^2 \frac{dN}{dS} dS \right)^{3/2}} \quad (12)$$

where S is the source flux, the integral runs up to the detection limit of the resolved sources indicated by a flux cut S_{cut} , and $\frac{dN}{dS}$ are the number counts per steradian.

This prescription gives a bispectrum in good agreement with the one measured on maps of radio and dusty star-forming galaxies simulated by Sehgal et al. (2010).

In the following, we will focus solely on IR point-sources. The level of non-Gaussianity induced by IR sources can thus be quantified by the amplitude of their bispectrum compared to the template bispectrum given by Eq.11. The use of the amplitude of the bispectrum permits to derive easily the bias on primordial CMB estimation f_{NL} , and to marginalise over this nuisance parameter as will be seen in Sect.5.

The amplitude of the bispectrum is measured by minimising the χ^2 of the map bispectrum to the theoretical one :

$$\chi^2(A) = \sum_{\ell_1 \leq \ell_2 \leq \ell_3} \frac{(\mathbf{b}_{1,2,3} - A \mathbf{b}_{1,2,3}^{\text{IR}})^2}{\sigma^2(\ell_1, \ell_2, \ell_3)} \quad (13)$$

with

$$\sigma^2(\ell_1, \ell_2, \ell_3) = \frac{C_{\ell_1}^{\text{tot}} C_{\ell_2}^{\text{tot}} C_{\ell_3}^{\text{tot}}}{N_{\ell_1 \ell_2 \ell_3}} \times \Delta_{\ell_1 \ell_2 \ell_3} \quad (14)$$

being the bispectrum variance in the weak non-Gaussianity limit¹. In this expression, C_ℓ^{tot} is the map power spectrum, and we have

$$\begin{aligned} \Delta_{\ell_1 \ell_2 \ell_3} &= 1 + \delta_{\ell_1 \ell_2} + \delta_{\ell_1 \ell_3} + \delta_{\ell_2 \ell_3} + 2 \delta_{\ell_1 \ell_2 \ell_3} \\ &= \begin{cases} 6 & \text{equilateral triangle} \\ 2 & \text{isosceles triangle} \\ 1 & \text{general triangle} \end{cases} \end{aligned} \quad (15)$$

Then the maximum likelihood estimator is:

$$\hat{A} = \sum_{\ell_1 \leq \ell_2 \leq \ell_3} \frac{\mathbf{b}_{1,2,3} \mathbf{b}_{1,2,3}^{\text{IR}}}{\sigma^2(\ell_1, \ell_2, \ell_3)} \times \sigma^{-2}(\hat{A}) \quad (16)$$

¹ This approximation is justified for the Cosmic Infrared Background (CIB) which is close to Gaussian (see (Lacasa et al. 2012) for details)

with

$$\sigma^2(\hat{A}) = \sum_{\ell_1 \leq \ell_2 \leq \ell_3} \frac{(\mathbf{b}_{1,2,3}^{\text{IR}})^2}{\sigma^2(\ell_1, \ell_2, \ell_3)} \quad (17)$$

being a normalisation factor giving the error-bar in the assumption of a Gaussian likelihood, which is valid in the weak NG limit when $\sigma^2(\ell_1, \ell_2, \ell_3)$ can be considered independent of A .

The theoretical bispectrum, Eq. 11, is separable²; hence a simpler computation of the numerator of Eq. 16 can be devised, inspired by Komatsu et al. (2005). Indeed, defining the filtered map:

$$F(\mathbf{n}) = \sum_{\ell m} \frac{\alpha^{1/3} \sqrt{C_\ell^{\text{IR}}} b_\ell}{C_\ell^{\text{tot}}} a_{\ell m} Y_{\ell m}(\mathbf{n}) \quad (18)$$

and

$$\mathcal{S}_{\text{IR}} = \int d^2 \mathbf{n} F(\mathbf{n})^3 \quad (19)$$

we have:

$$\mathcal{S}_{\text{IR}} = \sum_{\ell_1 \ell_2 \ell_3} \frac{\mathbf{b}_{1,2,3}^{\text{IR}} \hat{\mathbf{b}}_{123}}{C_{\ell_1}^{\text{tot}} C_{\ell_2}^{\text{tot}} C_{\ell_3}^{\text{tot}}} \times N_{123} = 6 \times \sum_{\ell_1 \leq \ell_2 \leq \ell_3} \frac{\mathbf{b}_{1,2,3}^{\text{IR}} \hat{\mathbf{b}}_{123}}{\sigma^2(\ell_1, \ell_2, \ell_3)} \quad (20)$$

Furthermore it is worth noting that this approach is faster than a full bispectrum analysis, having $O(N_{\text{pix}}^{3/2})$ operations.

3. Masked sky and inhomogeneous noise

In realistic cases of CMB analysis, the statistical isotropy of the CMB signal is broken by inhomogeneous noise –e.g. due to scanning strategy– or by masking large areas of the sky –e.g. those contaminated by galactic emissions. In these cases, the estimator of the IR-bispectrum amplitude is no longer optimal and it is biased in a non-trivial way. Nevertheless and similarly to the case of the f_{NL} , the bias and the lack of optimality can both be tackled through adapted modifications to the estimator.

3.1. Debiasing

When a covariance matrix of the map(s) can be estimated, Creminelli et al. (2006) have shown that Wiener filtering of the map(s) will debias the non-Gaussian estimator from anisotropic contaminants or noise. Specifically, if \mathbf{C} is the estimated covariance matrix in harmonic space, the estimator Eq. 16 can be debiased by making the change

$$a_{\ell m} \rightarrow (\mathbf{C}^{-1} \cdot \mathbf{a})_{\ell m} = \sum_{\ell' m'} C_{\ell m, \ell' m'}^{-1} a_{\ell' m'} \quad (21)$$

in the filtered map Eq. 18, where $\mathbf{a} = (a_{\ell m})_{\ell=2.. \ell_{\text{max}}, m=-\ell.. \ell}$ is the vector of harmonic coefficients.

This step is sometimes called \mathbf{C}^{-1} prefiltering, and replaces the $1/C_\ell^{\text{tot}}$ filtering of Eq. 18 (in the isotropic case \mathbf{C}^{-1} reduces to $1/C_\ell^{\text{tot}}$). An efficient algorithm for this filtering has been designed by Elsner & Wandelt (2012).

² a bispectrum is said separable if it can be written in the form $b(\ell_1, \ell_2, \ell_3) = \sum_i f_i(\ell_1) g_i(\ell_2) h_i(\ell_3) + \text{perm}$. This is the case for the IR bispectrum with the sum reducing to 1 element and $f_i(\ell) = g_i(\ell) = h_i(\ell) = \alpha^{1/3} \sqrt{C_\ell^{\text{IR}}}$

3.2. Reducing variance and reaching optimality

When isotropy is broken, the 3-point correlation function used to define the bispectrum in Eq. 6 no longer has minimal variance. It must be replaced by the Wick product of the three harmonic coefficients given by:

$$a_{\ell_1 m_1} a_{\ell_2 m_2} a_{\ell_3 m_3} \rightarrow a_{\ell_1 m_1} a_{\ell_2 m_2} a_{\ell_3 m_3} - \langle a_{\ell_1 m_1} a_{\ell_2 m_2} \rangle a_{\ell_3 m_3} - \langle a_{\ell_1 m_1} a_{\ell_3 m_3} \rangle a_{\ell_2 m_2} - \langle a_{\ell_2 m_2} a_{\ell_3 m_3} \rangle a_{\ell_1 m_1}. \quad (22)$$

This expression exhibits the same mean as in the isotropic case but it has a lower variance. Furthermore when applied to the isotropic case Eq. 22 gives the same bispectrum estimator as in Eq. 6 (e.g. for $\ell_1 \neq \ell_2 \neq \ell_3$ all the expectation values vanish).

Only the 2-point correlation function is to be considered for the expectation values. Therefore in practice, the latter are obtained from a sufficiently large number of Gaussian realisations with same power spectrum as that of the signal considered.

Inputting the linear corrections given by Eq. 22 into the expression of \mathcal{S}_{IR} in Eq. 20 yields:

$$\mathcal{S}_{\text{IR}} \rightarrow \tilde{\mathcal{S}}_{\text{IR}} = \int d^2 \mathbf{n} F(\mathbf{n})^3 - 3 \times \int d^2 \mathbf{n} F(\mathbf{n}) G(\mathbf{n}) \quad (23)$$

with

$$G(\mathbf{n}) = \sum_{12} \alpha^{2/3} \sqrt{C_{\ell_1}^{\text{IR}} C_{\ell_2}^{\text{IR}}} \langle a_1 a_2 \rangle_{\text{MC}} Y_1(\mathbf{n}) Y_2(\mathbf{n}) \quad (24)$$

$$= \langle F(\mathbf{n})^2 \rangle_{\text{MC}} \quad (25)$$

4. Expected detection significance

In this section, we present the expected detection significance in terms of the signal-to-noise ratio for the previously described estimator. To this end, we use values of α and C_ℓ^{IR} that we measure in the simulations of Sehgal et al. (2010) at frequencies 150, 220, 280 and 350 GHz. The obtained values were shown to reproduce adequately the IR bispectrum at these frequencies (see Lacasa et al. (2012)).

4.1. Ideal cosmic variance-limited case

Let us first focus on an ideal case where the signal is made solely of IR galaxies, i.e. noise and other astrophysical contributions are neglected. We will compute the signal-to-noise ratio of the detection of the non-Gaussian signal as defined by the amplitude of the bispectrum. Each triplet $\ell_1 \leq \ell_2 \leq \ell_3$ contains information proportional to its number of configurations :

$$\sigma^2(\hat{A}) = \alpha^2 \sum_{\ell_1 \leq \ell_2 \leq \ell_3} N_{\ell_1 \ell_2 \ell_3} \quad (26)$$

In other terms, the SNR of the detection goes down with the total number of bispectrum configurations:

$$\text{SNR} = \frac{1}{\sigma(\hat{A})} \propto 1 / \sqrt{N_{\text{tot}}(\ell_{\text{max}})} \quad (27)$$

with

$$N_{\text{tot}}(\ell_{\text{max}}) = \sum_{\ell_{\text{min}} \leq \ell_1 \leq \ell_2 \leq \ell_3 \leq \ell_{\text{max}}} N_{\ell_1 \ell_2 \ell_3} \quad (28)$$

For example in the case of full-sky maps of the IR sources at frequencies 150, 220, 280 and 350 GHz with angular scales ranging from $\ell_{\text{min}} = 2$ to $\ell_{\text{max}} = 2048$, the obtained SNRs are of order ~ 1000 and they do not vary much from frequency to frequency (see first line of Table 1).

4.2. Realistic case

In a real experiment, the IR signal/map is convolved by the instrumental beam and the signal is contaminated by noise and other astrophysical signals, the most prominent being the CMB and the galaxy, which can be masked. Hence the SNR is significantly decreased compared to the ideal case. Table 1 summarizes the expected SNR in the case of a 5 arcmin beam and 10^{-8} dT/T homogeneous detector noise across frequencies. We show how the detection level/significance decrease from the ideal case to the case of a convolved but "perfect" full-sky IR map, then including CMB contamination but still full-sky, and finally with a 50% sky-fraction mimicking the mask that may be applied to avoid galactic dust emission. We also include the case where 90% of the CMB can be removed by a component separation method. For the partial-sky coverage cases, we assume that the optimisation and the debiasing described in Sect. 3.1&3.2 have been applied with the SNR scaling as $f_{\text{SKY}}^{-1/2}$.

frequency (GHz)	150	220	280	350
Ideal case	1218	1157	1161	1159
Full-sky IR	15.5	98	336	833
Full-sky with CMB	0.39	6.7	55	387
50% sky with CMB	0.28	4.7	39	274
50% sky with 10% CMB	3.67	45.9	210	577

Table 1. Expected SNR at $\ell_{\text{max}} = 2048$. Ideal stands for a full-sky cosmic-variance limited IR map without noise nor contaminations. Full-sky IR represents the case where the IR map is convolved with a 5 arcmin Gaussian beam and contains 10^{-8} $\Delta T/T$ noise ($C_\ell = 7.4 \cdot 10^{-4} \mu K^2 \cdot \text{sr}$). The same instrumental specifications are adopted for the following lines. Full-sky with CMB is when CMB is present, contaminating the IR map. 50% sky with CMB stands for the case of masking half of the sky. 50% sky with 10% CMB stands for a half sky IR map where 90% of the CMB (in amplitude) has been removed by some component separation.

The SNR of the detection is severely reduced from ideal to more realistic cases especially at lower frequencies. The signal is still detectable at all frequencies when including beam and noise effects. However, when the CMB is included the signal becomes undetectable at 150 GHz. Above this frequency the detection significance is $\text{SNR} \sim 5\sigma$ at 220 GHz and reaches 40 to 200σ at 280 and 350 GHz where the IR emission is dominant even in presence of CMB contribution.

Removing the CMB, with a component separation method, permits to further improve the detection at 220 GHz by increasing the SNR to $\sim 46\sigma$. In this case, the IR non-Gaussianity at 150 GHz seems marginally detectable. However at this frequency the non-Gaussianity from radio sources becomes an issue (while at higher frequencies IR sources are forecasted to dominate the unresolved sources population). We tackle in the next section the issue of non-Gaussianity other than that of the IR sources.

5. Joint NG estimation

When several non-Gaussian signals are present, a joint estimation of their amplitudes taking their covariances into account is necessary. We focus in the present study on the main extragalactic non-Gaussian signals, namely CMB, radio and IR

point-sources. A joint estimation requires minimisation of the chi-square :

$$\chi^2(f_{\text{NL}}, b_{\text{PS}}, A_{\text{IR}}) = \sum_{\ell_1 \leq \ell_2 \leq \ell_3} \frac{(\mathbf{b}_{1,2,3}^{\text{obs}} - \mathbf{b}_{1,2,3}^{\text{model}}(f_{\text{NL}}, b_{\text{PS}}, A_{\text{IR}}))^2}{\sigma^2(\ell_1, \ell_2, \ell_3)} \quad (29)$$

with

$$\mathbf{b}_{1,2,3}^{\text{model}}(f_{\text{NL}}, b_{\text{PS}}, A_{\text{IR}}) = f_{\text{NL}} \mathbf{b}_{1,2,3}^{\text{CMB}} + b_{\text{PS}} \mathbf{b}_{1,2,3}^{\text{RAD}} + A_{\text{IR}} \mathbf{b}_{1,2,3}^{\text{IR}} \quad (30)$$

and (involved in the definition of $\sigma^2(\ell_1, \ell_2, \ell_3)$, see Eq.14)

$$C_\ell^{\text{tot}} = (C_\ell^{\text{CMB}} + C_\ell^{\text{RAD}} + C_\ell^{\text{IR}}) b_\ell^2 + C_\ell^{\text{noise}} \quad (31)$$

We use the standard' parameter b_{PS} for compatibility with the literature (instead of noting e.g. A_{RAD}).

Then if we define the scalar product between two bispectra \mathbf{b}^α and \mathbf{b}^β :

$$\langle \mathbf{b}^\alpha, \mathbf{b}^\beta \rangle = \sum_{\ell_1 \leq \ell_2 \leq \ell_3} \frac{\mathbf{b}_{1,2,3}^\alpha \mathbf{b}_{1,2,3}^\beta}{\sigma^2(\ell_1, \ell_2, \ell_3)} \quad (32)$$

Minimising Eq.29 corresponds to solving the linear system :

$$\begin{pmatrix} \langle \mathbf{b}_{\text{CMB}}, \mathbf{b}_{\text{CMB}} \rangle & \langle \mathbf{b}_{\text{RAD}}, \mathbf{b}_{\text{CMB}} \rangle & \langle \mathbf{b}_{\text{IR}}, \mathbf{b}_{\text{CMB}} \rangle \\ \langle \mathbf{b}_{\text{CMB}}, \mathbf{b}_{\text{RAD}} \rangle & \langle \mathbf{b}_{\text{RAD}}, \mathbf{b}_{\text{RAD}} \rangle & \langle \mathbf{b}_{\text{IR}}, \mathbf{b}_{\text{RAD}} \rangle \\ \langle \mathbf{b}_{\text{CMB}}, \mathbf{b}_{\text{IR}} \rangle & \langle \mathbf{b}_{\text{RAD}}, \mathbf{b}_{\text{IR}} \rangle & \langle \mathbf{b}_{\text{IR}}, \mathbf{b}_{\text{IR}} \rangle \end{pmatrix} \cdot \begin{pmatrix} f_{\text{NL}} \\ b_{\text{PS}} \\ A_{\text{IR}} \end{pmatrix} = \begin{pmatrix} \langle \mathbf{b}_{\text{obs}}, \mathbf{b}_{\text{CMB}} \rangle \\ \langle \mathbf{b}_{\text{obs}}, \mathbf{b}_{\text{RAD}} \rangle \\ \langle \mathbf{b}_{\text{obs}}, \mathbf{b}_{\text{IR}} \rangle \end{pmatrix} \quad (33)$$

If we introduce –noted with upper tilde– the "naive" estimators which consider only one source of non-Gaussianity, e.g.

$$\tilde{A}_{\text{IR}} = \frac{\langle \mathbf{b}_{\text{obs}}, \mathbf{b}_{\text{IR}} \rangle}{\langle \mathbf{b}_{\text{IR}}, \mathbf{b}_{\text{IR}} \rangle} \quad (34)$$

then Eq.33 can be rewritten to define the Joint NG estimators –noted with upper hat– as :

$$\begin{pmatrix} \hat{f}_{\text{NL}} \\ \hat{b}_{\text{PS}} \\ \hat{A}_{\text{IR}} \end{pmatrix} = \mathcal{M}^{-1} \cdot \begin{pmatrix} \tilde{f}_{\text{NL}} \\ \tilde{b}_{\text{PS}} \\ \tilde{A}_{\text{IR}} \end{pmatrix} \quad (35)$$

with

$$\mathcal{M} = \begin{pmatrix} 1 & \Delta f_{\text{NL}}^{\text{RAD}} & \Delta f_{\text{NL}}^{\text{IR}} \\ \Delta b_{\text{PS}}^{\text{CMB}} & 1 & \Delta b_{\text{PS}}^{\text{IR}} \\ \Delta A_{\text{IR}}^{\text{CMB}} & \Delta A_{\text{IR}}^{\text{RAD}} & 1 \end{pmatrix} \quad (36)$$

and

$$\begin{aligned} \Delta f_{\text{NL}}^{\text{RAD}} &= \frac{\langle \mathbf{b}_{\text{RAD}}, \mathbf{b}_{\text{CMB}} \rangle}{\langle \mathbf{b}_{\text{CMB}}, \mathbf{b}_{\text{CMB}} \rangle} & \Delta f_{\text{NL}}^{\text{IR}} &= \frac{\langle \mathbf{b}_{\text{IR}}, \mathbf{b}_{\text{CMB}} \rangle}{\langle \mathbf{b}_{\text{CMB}}, \mathbf{b}_{\text{CMB}} \rangle} \\ \Delta b_{\text{PS}}^{\text{CMB}} &= \frac{\langle \mathbf{b}_{\text{CMB}}, \mathbf{b}_{\text{RAD}} \rangle}{\langle \mathbf{b}_{\text{RAD}}, \mathbf{b}_{\text{RAD}} \rangle} & \Delta b_{\text{PS}}^{\text{IR}} &= \frac{\langle \mathbf{b}_{\text{IR}}, \mathbf{b}_{\text{RAD}} \rangle}{\langle \mathbf{b}_{\text{RAD}}, \mathbf{b}_{\text{RAD}} \rangle} \\ \Delta A_{\text{IR}}^{\text{CMB}} &= \frac{\langle \mathbf{b}_{\text{CMB}}, \mathbf{b}_{\text{IR}} \rangle}{\langle \mathbf{b}_{\text{IR}}, \mathbf{b}_{\text{IR}} \rangle} & \Delta A_{\text{IR}}^{\text{RAD}} &= \frac{\langle \mathbf{b}_{\text{RAD}}, \mathbf{b}_{\text{IR}} \rangle}{\langle \mathbf{b}_{\text{IR}}, \mathbf{b}_{\text{IR}} \rangle} \end{aligned}$$

We compute for illustration the mixing matrix at 220 GHz. Neglecting the noise and beam effect and assuming the ERCSC flux cuts (Planck Collaboration et al. 2011a), we find for $\ell_{\text{max}} = 2048$:

$$\mathcal{M} = \begin{pmatrix} 1 & 0.124 & 0.631 \\ 2.08 \cdot 10^{-5} & 1 & 1.79 \\ 3.16 \cdot 10^{-5} & 0.535 & 1 \end{pmatrix} \quad (37)$$

where we renormalised the radio amplitude to get numbers of order 1, i.e., the mixing matrix must be understood to be applied to $b_{\text{PS}}/(1.8 \cdot 10^{-28})$.

The matrix is mostly bloc diagonal, with the f_{NL} part decoupling from the b_{PS} and A_{IR} parts. Therefore, unless $b_{\text{PS}} \gg 10^{-28}$, f_{NL} estimation can be considered unaffected by extragalactic foregrounds at this frequency. Conversely, estimation of NG from radio and IR is unaffected by f_{NL} , but however we see that the two contributions affect heavily each other, with the $b_{\text{PS}}-A_{\text{IR}}$ submatrix being poorly conditioned (condition number ~ 180).

When we include instrumental effects, namely a 5 arcmin Gaussian beam and a $10^{-8} \Delta T/T$ noise (same ℓ_{max} and flux cut), we find the mixing matrix :

$$\mathcal{M} = \begin{pmatrix} 1 & 0.0461 & 0.245 \\ 1.21 \cdot 10^{-4} & 1 & 2.12 \\ 1.31 \cdot 10^{-4} & 0.435 & 1 \end{pmatrix} \quad (38)$$

The relative importance of CMB NG compared to point-sources NG has increased. Indeed beam and noise effects mostly decrease the signal-to-noise in configurations with high multipoles ; this down-weights point-sources NG which is dominant at high ℓ , while CMB NG dominates at lower multipoles. However CMB and point-sources NG estimation can still be considered decoupled unless $b_{\text{PS}} \gg 10^{-28}$. In the $b_{\text{PS}}-A_{\text{IR}}$ submatrix, we see that the relative importance of b_{PS} has decreased compared to A_{IR} . Indeed the IR signal is most important at large angular scales while the radio SNR comes mostly from small angular scales which are affected by the beam smoothing and the noise.

The $b_{\text{PS}}-A_{\text{IR}}$ submatrix is still ill-conditioned when we account for beam and noise effect ; this is due to a high correlation between the IR and radio bispectrum templates. This correlation can be quantified by the quantity $r = \cos \theta \in [-1, 1]$:

$$r_{\alpha\beta} = \frac{\langle \mathbf{b}_\alpha, \mathbf{b}_\beta \rangle}{\sqrt{\langle \mathbf{b}_\alpha, \mathbf{b}_\alpha \rangle \langle \mathbf{b}_\beta, \mathbf{b}_\beta \rangle}} \quad (39)$$

with $\alpha, \beta = \text{RAD,IR or CMB}$. In other terms $\theta_{\alpha\beta}$ is the angle between the vectors $\mathbf{b}_\alpha, \mathbf{b}_\beta$ in the vector space of bispectra with the scalar product defined in Eq.32. At $\ell_{\text{max}} = 2048$, with a 5 arcmin Gaussian beam and $10^{-8} \Delta T/T$ noise, the correlation coefficients of the different bispectra are listed in Table 2.

	IR/RAD	IR/CMB	RAD/CMB
r	96%	0.57%	0.24%

Table 2. Correlation coefficients between the different bispectrum templates at 220 GHz with $\ell_{\text{max}} = 2048$, 5 arcmin Gaussian beam and $10^{-8} \Delta T/T$ noise.

In Fig.1, we plot these coefficients as a function of the maximum multipole used in the analysis, with the same instrumental specifications.

When analysing only large angular scales (small ℓ_{max}), the radio and IR bispectrum templates are anti-correlated with the CMB bispectrum. This is because both radio and IR bispectra estimators are positive while the CMB is negative due to the Sachs-Wolfe effect term. However when going to higher resolution, the first acoustic peak makes the CMB bispectrum positive with large values in some configurations (e.g. equilateral). This makes the correlation between the radio and CMB bispectrum positive for $\ell \geq 168$. The IR/CMB correlation in turn, becomes positive at slightly higher multipoles, $\ell = 190$, because the IR bispectrum peaks in the squeezed configurations where the CMB

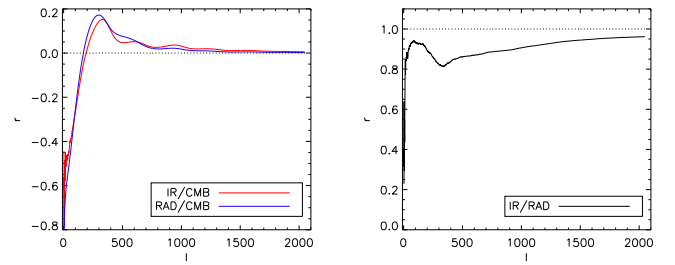


Figure 1. Correlation coefficients between the radio, IR and CMB bispectra at 220 GHz with 5 arcmin Gaussian beam and $10^{-8} \Delta T/T$ noise. Left panel : correlation between IR and CMB in red, between radio and CMB in blue, as a function of ℓ_{max} . Right panel : correlation between IR and radio.

bispectrum is still negative. At larger multipoles, because of the complex pattern of the CMB bispectrum and the changes of sign with acoustic peaks, the correlation coefficients tend asymptotically to zero.

The IR and radio bispectrum templates are positively correlated as they are both positive ; this correlation is small when analysing only the lowest multipoles, but it increases rapidly over 80% with a small 'dip' at $\ell_{\text{max}} = 200 - 300$ at the location of the first CMB acoustic peak. Indeed the CMB spectrum is involved in the denominator of Eq.32, so at $\ell_{\text{max}} = 200 - 300$ it typically down-weights non-squeezed configurations where radio and IR bispectra are the most correlated. Nevertheless, the correlation between radio and IR bispectra asymptotically tends to 1 at high angular resolutions, as the IR bispectrum flattens at high multipoles.

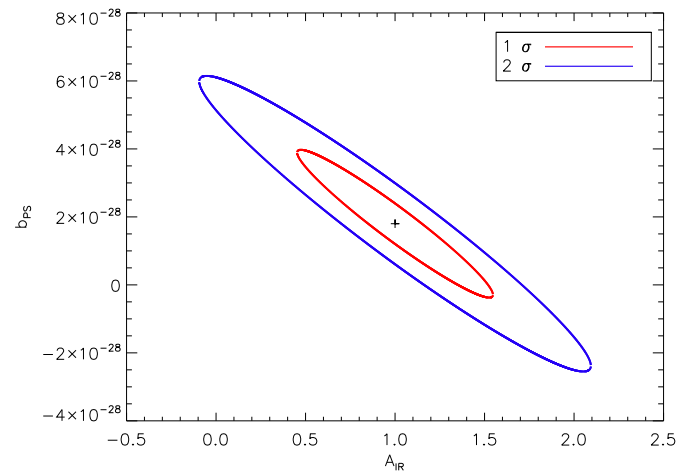


Figure 2. 1σ and 2σ confidence level for $(A_{\text{IR}}, b_{\text{PS}})$ in a joint estimation at 220 GHz $\ell_{\text{max}} = 2048$ with 5 arcmin Gaussian beam and $10^{-8} \Delta T/T$ noise

Finally, in Fig.2 we forecast the likelihood contours in the $(A_{\text{IR}}, b_{\text{PS}})$ plane, that we expect with the aforementioned instrumental specifications. A_{IR} and b_{PS} estimations are quite degenerate, as expected from the high correlations of their templates, which significantly degrades the constrain that can be put on each of them independently. However we can still have an order of magnitude estimation for both of them. Also, including

the prior $b_{\text{PS}} \geq 0$ (and also to some extent $A_{\text{IR}} \geq 0$) would improve the constraints. Finally, CMB removal through component separation may also help by decreasing the variance of both estimators (although not their correlation).

6. Conclusions and discussion

The prescription proposed in Lacasa et al. (2012) yields a separable form for the bispectrum of IR point-sources. This permits us to build a fast estimator for its amplitude à-la-KSW (Komatsu et al. 2005). We show how this estimator can be optimised to account for partial sky coverage and inhomogeneous noise. We compute the detection significance that can be expected at several frequencies. Finally we show how this estimator can be used together with estimators of the radio and CMB non-Gaussianity to build a joint estimation of sources of non-Gaussianity. We find that the estimation of CMB NG is barely correlated with the estimation of point-sources NG, so that unless the latter is too important –e.g. if few sources are masked–, both estimations can be considered decoupled. On the contrary, for point-sources, IR and radio NG have similar shapes especially at high multipoles which make their amplitude estimation degenerate. We show how this hampers the detectability of the IR NG at 220 GHz. Increasing this detectability can be achieved for example by subtraction of the CMB, or by including priors on b_{PS} in the analysis (e.g. positivity and/or upper limits given the flux cut and radio source models).

This study opens up the possibility of robust measurements of non-Gaussianity where contaminations are treated in a systematic way. It also opens up the possibility of the detection of point-sources NG, which may permit to constrain their respective models.

Acknowledgments

The authors thank B. Wandelt for interesting discussions. They acknowledge the use of the HEALpix package (Gorski et al. 2005)

References

Acquaviva, V., Bartolo, N., Matarrese, S., & Riotto, A. 2003, Nuclear Physics B, 667, 119
 Babich, D. & Pierpaoli, E. 2008, Physical Review D, 77
 Creminelli, P., Nicolis, A., Senatore, L., Tegmark, M., & Zaldarriaga, M. 2006, Journal of Cosmology and Astroparticle Physics, 2006, 004
 Creminelli, P. & Zaldarriaga, M. 2004, Journal of Cosmology and Astroparticle Physics, 2004, 006
 Das, S., Marriage, T. A., Ade, P. A. R., et al. 2011, The Astrophysical Journal, 729, 62
 Elsner, F. & Wandelt, B. D. 2012, ArXiv e-prints
 González-Nuevo, J., Toffolatti, L., & Argüeso, F. 2005, ApJ, 621, 1
 Gorski, K. M., Hivon, E., Banday, A. J., et al. 2005, The Astrophysical Journal, 622, 759
 Hall, N. R., Keisler, R., Knox, L., et al. 2010, ApJ, 718, 632
 Keisler, R., Reichardt, C. L., Aird, K. A., & et al. 2011, The Astrophysical Journal, 743, 28
 Komatsu, E., Dunkley, J., Nolta, M. R., et al. 2009, ApJS, 180, 330
 Komatsu, E., Smith, K. M., Dunkley, J., et al. 2011, ApJS, 192, 18
 Komatsu, E., Spergel, D. N., & Wandelt, B. D. 2005, The Astrophysical Journal, 634, 14
 Lacasa, F., Aghanim, N., Kunz, M., & Frommert, M. 2012, Monthly Notices of the Royal Astronomical Society, 421, 1982
 Maldacena, J. 2003, Journal of High Energy Physics, 2003, 013
 Planck Collaboration. 2006, ArXiv Astrophysics e-prints
 Planck Collaboration, Ade, P. A. R., Aghanim, N., et al. 2011a, A&A, 536, A7
 Planck Collaboration, Ade, P. A. R., Aghanim, N., et al. 2011b, A&A, 536, A18
 Sehgal, N., Bode, P., Das, S., et al. 2010, The Astrophysical Journal, 709, 920